

## Supporting Information for

### ORIGINAL ARTICLE

## **Pulmonary endothelium-targeted nanoassembly of indomethacin and superoxide dismutase relieves lung inflammation**

**Yi Yang<sup>a,b,†</sup>, Makhloufi Zoulikha<sup>a,b,†</sup>, Qingqing Xiao<sup>b,c,†</sup>, Feifei Huang<sup>b</sup>, Qi Jiang<sup>b</sup>, Xiaotong Li<sup>b</sup>, Zhenfeng Wu<sup>d,\*</sup>, Wei He<sup>a,b,\*</sup>**

<sup>a</sup>*Shanghai Skin Disease Hospital, Tongji University School of Medicine, Shanghai 200443, China*

<sup>b</sup>*School of Pharmacy, China Pharmaceutical University, Nanjing 2111198, China*

<sup>c</sup>*Department of Traditional Chinese Medicine Processing and Preparation, Nanjing University of Chinese Medicine, Nanjing 210023, China*

<sup>d</sup>*Key Laboratory of Modern Preparation of TCM, Ministry of Education, Jiangxi University of Chinese Medicine, Nanchang 330004, China*

Received 2 February 2023; received in revised form 5 May 2023; accepted 6 May 2023

<sup>†</sup>These authors made equal contributions to this work.

\*Corresponding authors.

E-mail addresses: [zfwu527@163.com](mailto:zfwu527@163.com) (zhenfeng Wu), [weihe@cpu.edu.cn](mailto:weihe@cpu.edu.cn) (Wei He).

Running title: Pulmonary endothelium-targeted nanoassembly relieves lung inflammation

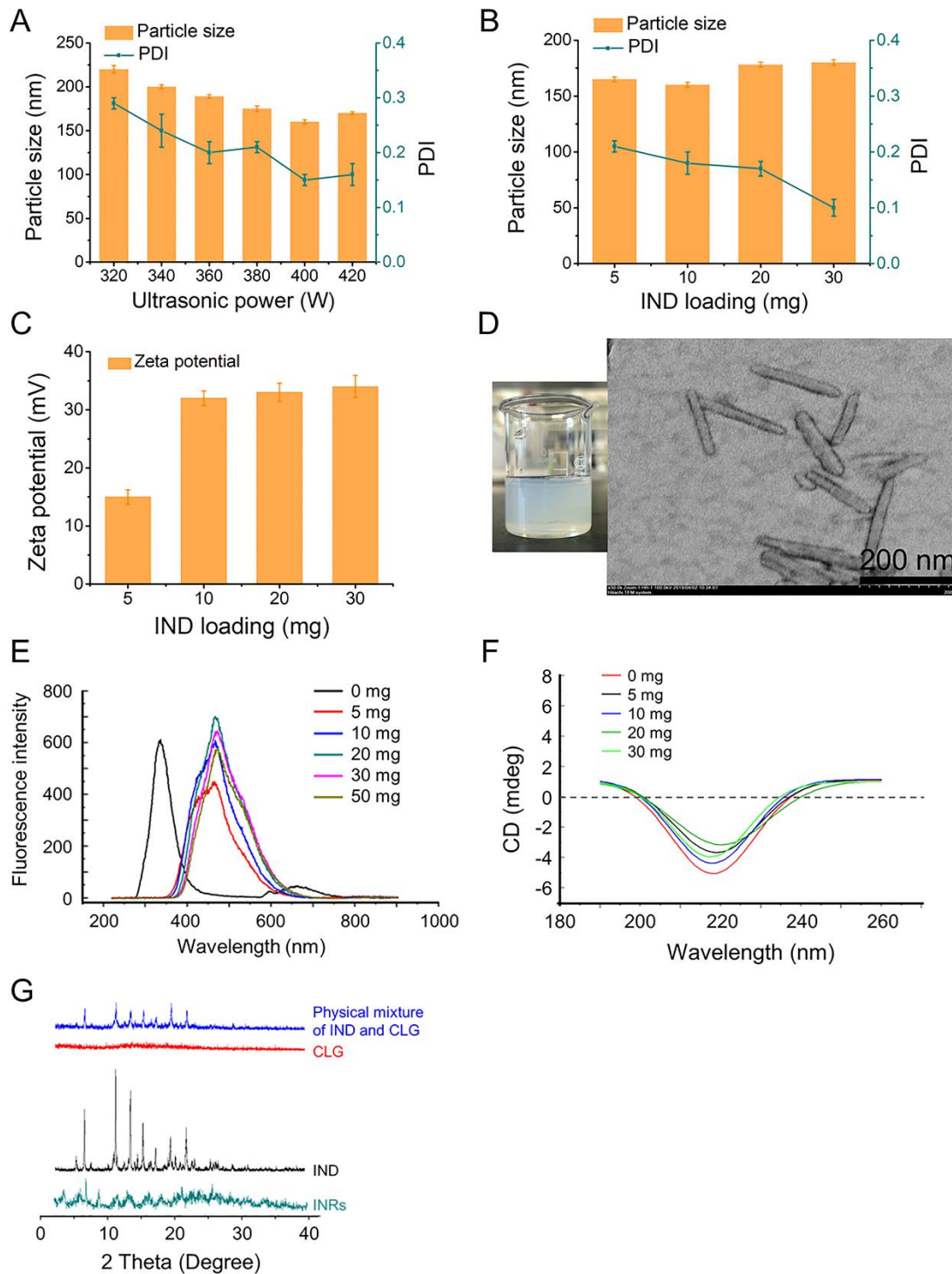


**Figure S1** Preparation and characterization of INRs. (A) The effect of ultrasonication power on the particle size of INRs. (B) Particle size and (C) zeta potential of INRs with different IND loadings. (D) TEM examination. (E) Fluorescent and (F) CD spectra of INRs with varying loadings of IND. (G) PXRD test. The data are expressed as mean  $\pm$  SD,  $n = 3$ .

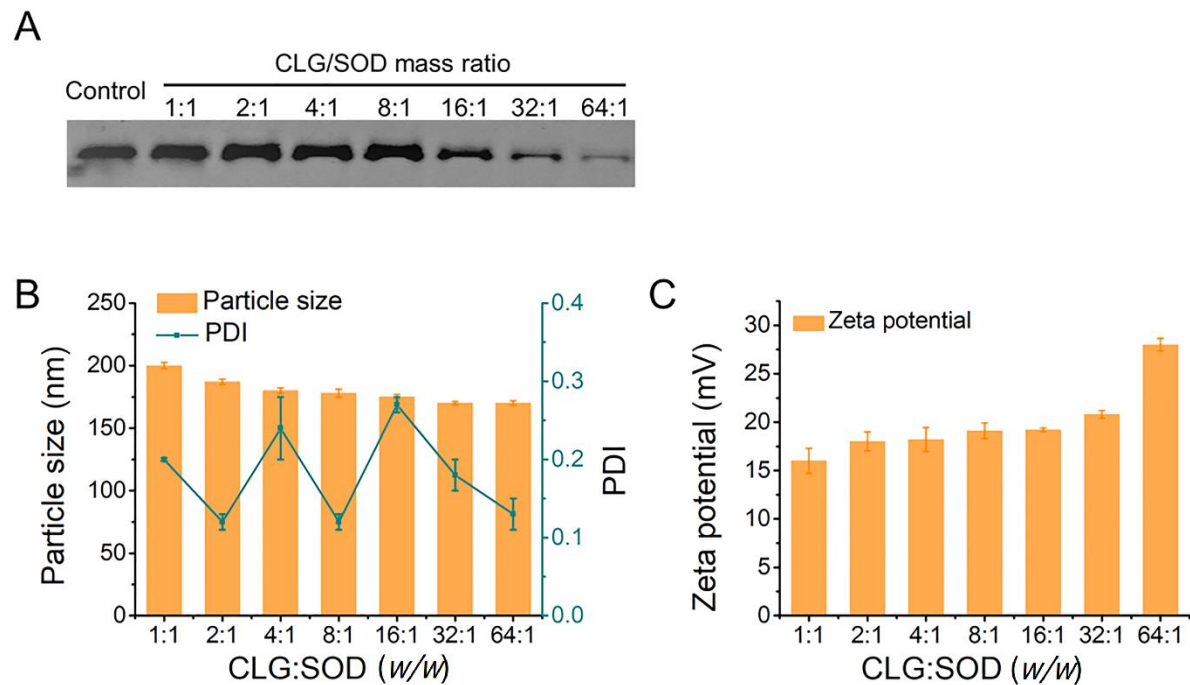


**Figure S2** Preparation and characterization of INRplex. (A) Gel electrophoresis of INRplex with different SOD loadings. (B) Particle size and (C) zeta potential of INRplex with different CLG:SOD mass ratios. The data are expressed as mean  $\pm$  SD,  $n = 3$ .

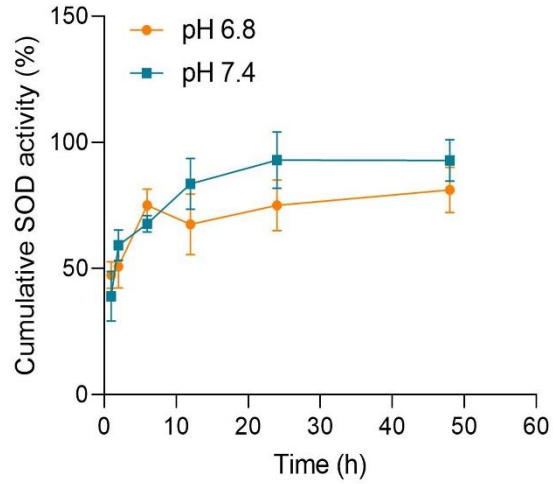


**Figure S3** SOD-activity determination during release study. The enzyme activity was determined during the *in vitro* release study of Ab-INRplex at pH 7.4 and 6.8, using the total SOD activity test kit. The naked SOD solution having 100% activity was utilized as a control containing an equivalent SOD dose to the preparation. The data are expressed as mean  $\pm$  SD,  $n = 3$ .

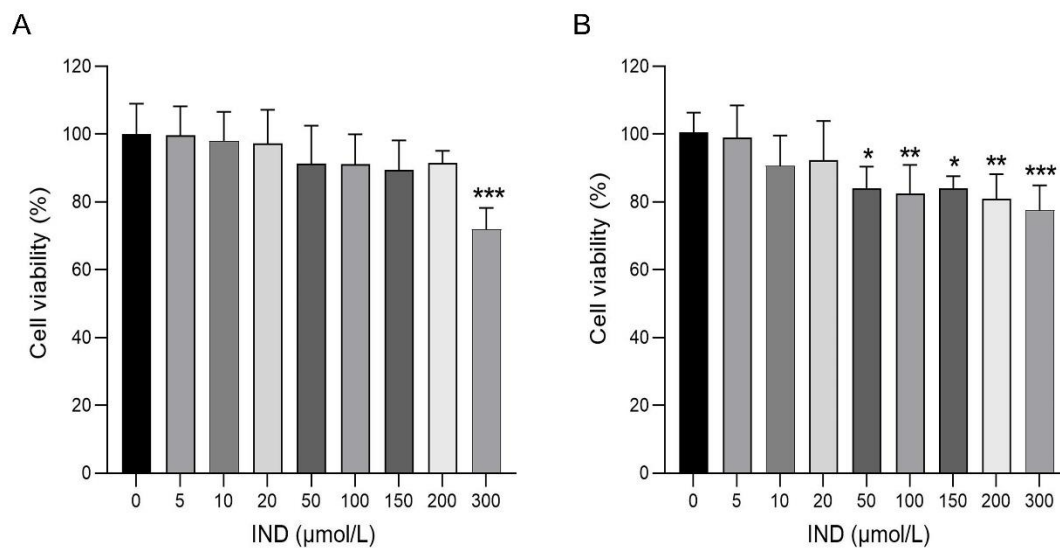


**Figure S4** Cell viability of HUVECs (A) and PASMCs (B) using MTT assay after INR treatment for 24 h with the optimized formulation containing different concentrations of IND. The data are expressed as mean  $\pm$  SD,  $n = 5$ , \* $P < 0.05$ , \*\* $P < 0.01$ , \*\*\* $P < 0.001$ , compared with the control group. Even at the incubation concentration of 200  $\mu\text{M}$ , the cell viability remained greater than 85%, indicating low cytotoxicity.

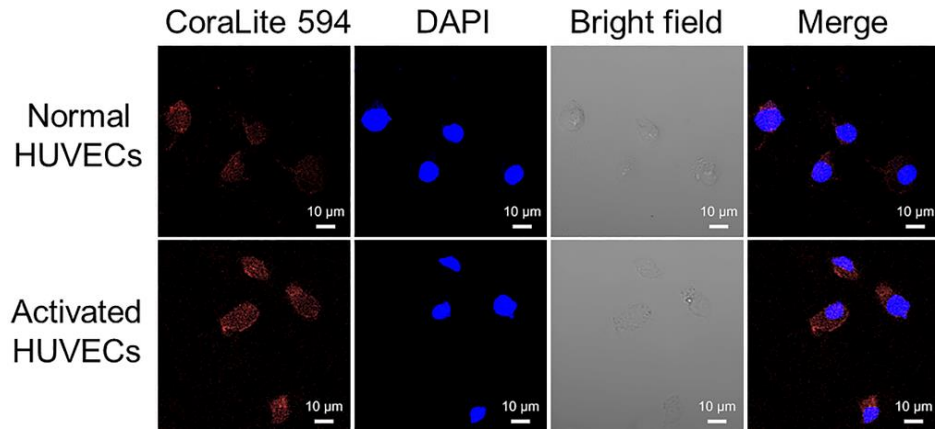


**Figure S5** CLSM examination of ICAM-1 expression on LPS-activated HUVECs compared with HUVECs. ICAM-1 primary antibody (1:100) was added and incubated at 4 °C overnight; CoraLite 594 fluorescent-labeled goat anti-mouse secondary antibody (1:1000) was incubated in the dark at 37 °C for 1 h.

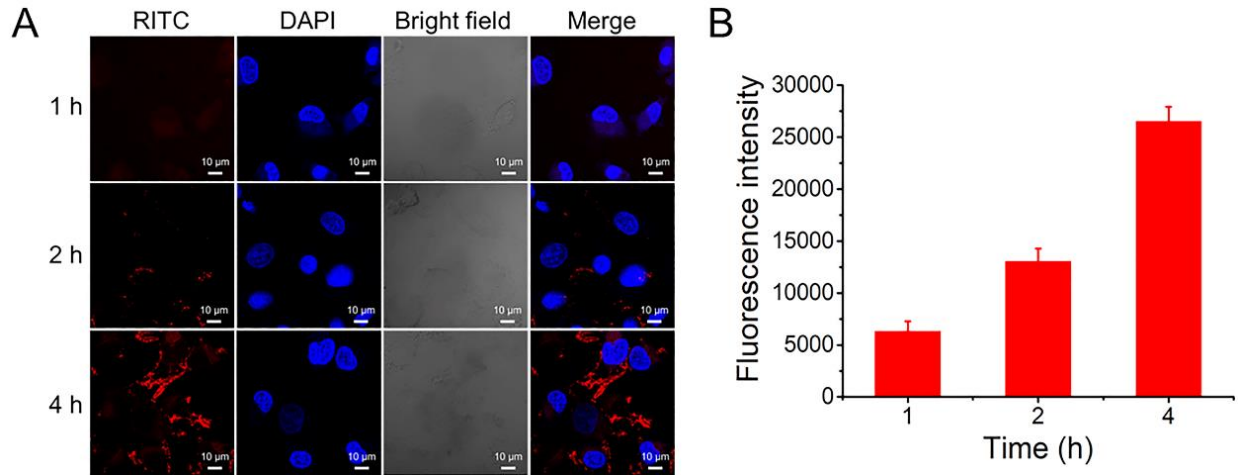


**Figure S6** Time-dependent cellular uptake of RITC-Ab-INRplex by LPS-activated HUVECs measured by (A) CLSM and quantitated by (B) flow cytometry. The cells were activated with LPS (2.5  $\mu\text{g}/\text{mL}$ ) for 2 h and treated with fluorescent Ab-INRplex at a RITC concentration of 10  $\mu\text{g}/\text{mL}$ . The cells were fixed with 4% paraformaldehyde and nuclei were stained with DAPI. Scale bar: 10  $\mu\text{m}$ . The data are expressed as mean  $\pm$  SD,  $n = 3$ .

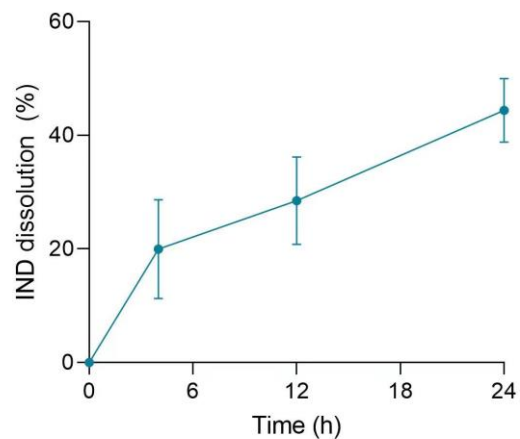


**Figure S7** IND dissolution from Ab-INRplex after cellular uptake. The intracellular drug concentration was determined by the HPLC method at 4, 12, and 24 h after incubation at 37 °C. The data are expressed as mean  $\pm$  SD,  $n = 3$ .



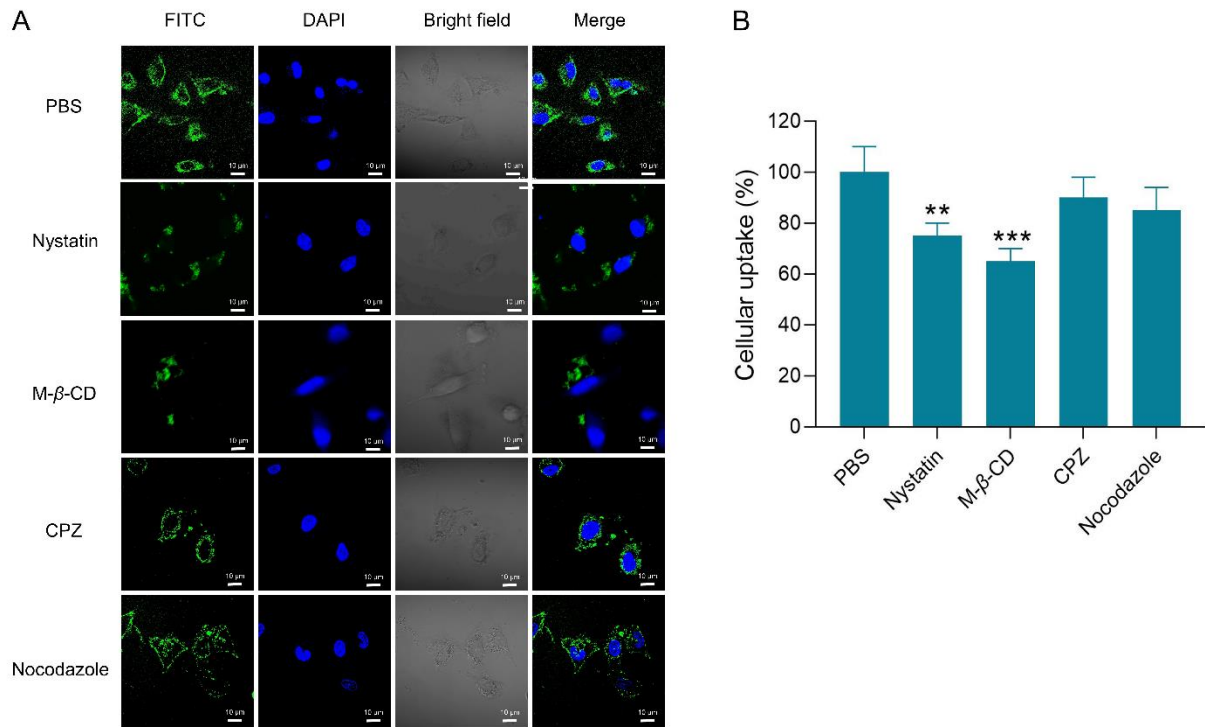


**Figure S8** Internalization mechanism of Ab-INRplex by LPS-activated HUVECs. (A) CLSM and (B) flow cytometry determination of cellular uptake of FITC-labeled Ab-INRplex after pre-incubation with endocytosis inhibitors for 30 min.  $n = 3$ ,  $**P < 0.01$ ,  $***P < 0.001$ , compared with PBS. Scale bar: 10  $\mu\text{m}$ .

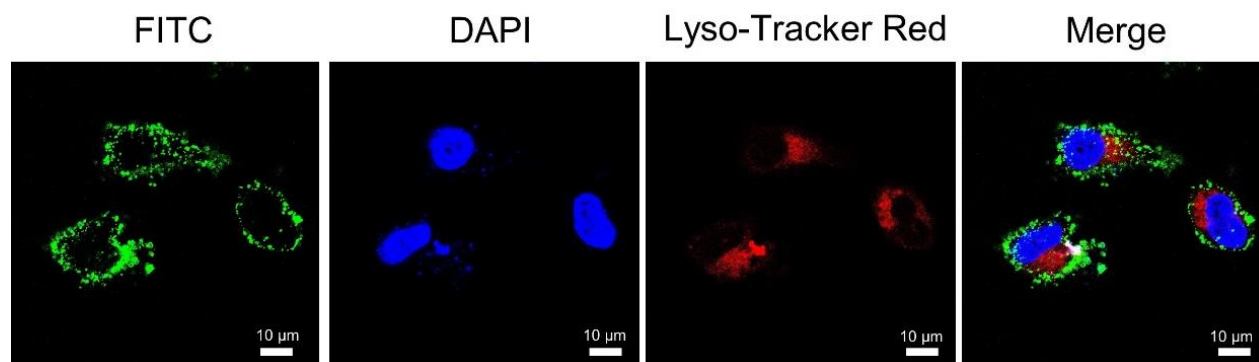


**Figure S9** Lysosomal localization of Ab-INRplex in the LPS-activated HUVECs observed under CLSM. The cells were activated with LPS (2.5 μg/mL) for 2 h and treated with FITC-Ab-INRplex at a FITC concentration of 7.5 μg/mL for 4 h. The cells were fixed with 4% paraformaldehyde and stained with Lyso-Tracker Red and DAPI, respectively. Scale bar: 10 μm.

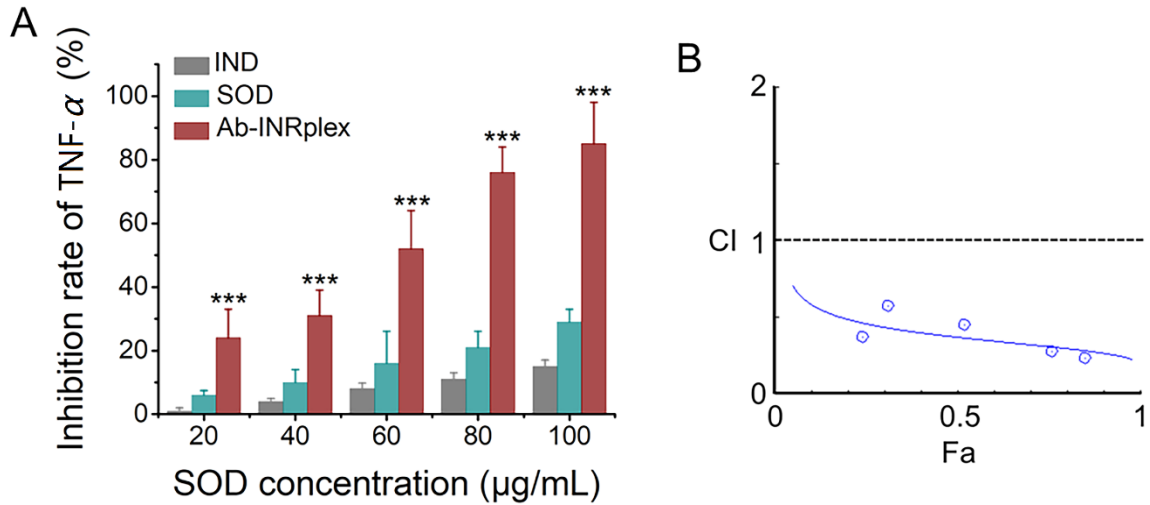


**Figure S10** Synergism between IND and SOD. (A) The expression of TNF- $\alpha$  in LPS-activated HUVECs after treatment with IND, SOD, or Ab-INRplex. (B) Combination index (CI)-fraction affected (Fa) plot of Ab-INRplex generated by CompuSyn software version 1.0. HUVECs were activated with LPS (2.5  $\mu\text{g}/\text{mL}$ ) for 2 h before treatment with preparations containing different concentrations of SOD (20, 40, 60, 80, 100  $\mu\text{g}/\text{mL}$ ) for 4 h. The data are expressed as mean  $\pm$  SD,  $n = 3$ , \*\*\* $P < 0.001$ , compared with free SOD or IND groups.

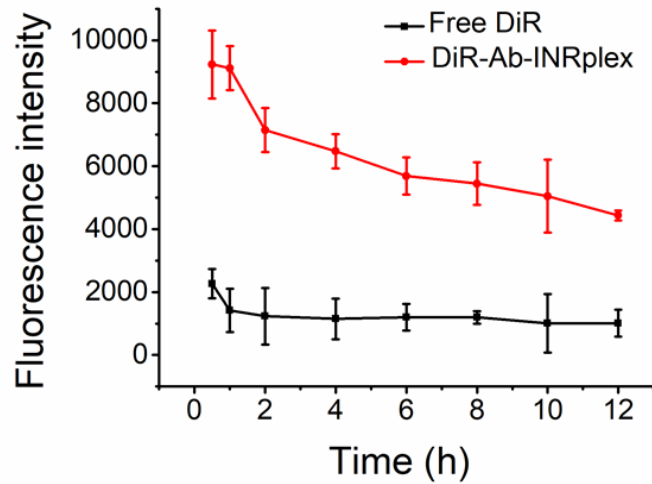


**Figure S11** DiR plasma concentration-time curves of free DiR and DiR-labeled Ab-INRplex. The LPS-induced ALI mice ( $n = 5$ ) were intravenously injected with free DiR and DiR-Ab-INRplex at a DiR dose of 1.5 mg/kg. The blood was collected at predetermined time intervals and the fluorescence intensity was detected by a multi-function microplate reader (ex: 730 nm; em: 790 nm). The data are expressed as mean  $\pm$  SD,  $n = 5$ .



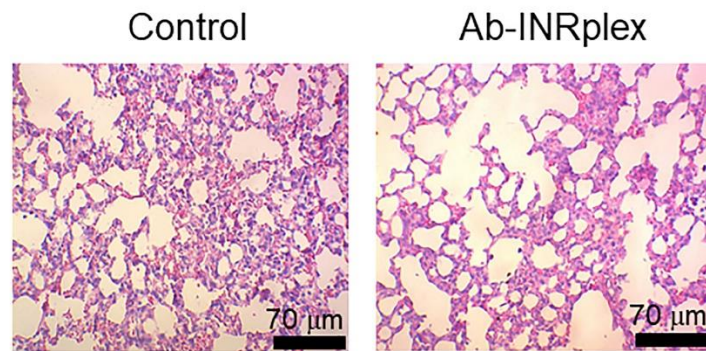


**Figure S13** H&E-stained lung sections. The lung tissues were collected from normal mice at 6 h after a single intravenous injection of saline or Ab-INRplex. The dose of IND/SOD was 4.8/0.15 mg/kg, according to the body weight.

**Table S1** The grafting efficacy of Ab attached to INRplex

Item	Feeded amount of Ab (per 1 mg INRplex)				
	7.5 $\mu$ g	15 $\mu$ g	30 $\mu$ g	60 $\mu$ g	120 $\mu$ g
Amount of attached Ab ( $\mu$ g)	3.0 $\pm$ 0.15	13.0 $\pm$ 0.2	20 $\pm$ 1.4	45.0 $\pm$ 5.1	83.0 $\pm$ 3.5
Grafting efficacy (%)	40.0 $\pm$ 2.0	86.7 $\pm$ 1.3	66.7 $\pm$ 4.8	75.0 $\pm$ 8.5	69.2 $\pm$ 2.9

Ab, anti-ICAM-1 antibody. The data are expressed as mean  $\pm$  SD,  $n = 3$ .